LEVEL II

N00014-75-C-1015

TOLERANCE OF THE NECK TO INDIRECT IMPACT

A. I. KING
WAYNE STATE UNIVERSITY
BIOENGINEERING CENTER
THE LOUIS SCIENCES BUILDING
DETROIT, MICHIGAN 48202

APRIL 5, 1979

TECHNICAL REPORT NO. 10

DEPARTMENT OF THE NAVY
OFFICE OF NAVAL RESEARCH
BIOLOGICAL SCIENCES PROGRAM (CODE 474)
ARLINGTON, VIRGINIA 22217

SECURITY CLASSIFICATION OF THIS PAGE (When Data Entered)

REPORT DOCUMENTATION PAGE

READ INSTRUCTIONS BEFORE COMPLETING FORM

1. REPORT NUMBER: N00014-75-C-1015	2. GOVT ACCESSION NO.
3. RECIPIENT'S CATALOG NUMBER	
4. TITLE (and Subtitle): Tolerance of the Neck to Indirect Impact. AD667971	5. TYPE OF REPORT & PERIOD COVERED: Technical Report No. 10
6. PERFORMING ORG. REPORT NUMBER	
7. AUTHOR(s): Albert I. King, Said S. Nakhla, Naveen K. Mital	8. CONTRACT OR GRANT NUMBER(s): N00014-75-C-1015
9. PERFORMING ORGANIZATION NAME AND ADDRESS: Department of the Navy, Office of Naval Research, Structural Mechanics Program (Code 474), Arlington, VA 22217	10. PROGRAM ELEMENT, PROJECT, TASK AREA & WORK UNIT NUMBERS: NR 064-524/12-10-75
11. CONTROLLING OFFICE NAME AND ADDRESS	12. REPORT DATE: March 5, 1979
	13. NUMBER OF PAGES: 16
14. MONITORING AGENCY NAME & ADDRESS (if different from Controlling Office): same as above	15. SECURITY CLASS. (of this report): Unclassified
	15a. DECLASSIFICATION/DOWNGRADING SCHEDULE

16. DISTRIBUTION STATEMENT (of this Report)

Approved for public release; distribution unlimited.

17. DISTRIBUTION STATEMENT (of the abstract entered in Block 20, if different from Report)

published in the proceedings of the Advisory Group for Aerospace Research and Development (North Atlantic Treaty Organization) entitled, "Models and Analogues for the Evaluation of Human Biodynamic Response, Performance and Protection". Meeting held in Paris, France, November 6-10, 1978

18. SUPPLEMENTARY NOTES

19. KEY WORDS (Continue on reverse side if necessary and identify by block number)

mathematical model of the spine, biodynamic response, $+G_z$ and $-G_x$ acceleration protective helmets, spinal cord injury

20. ABSTRACT (Continue on reverse side if necessary and identify by block number)

A two-dimensional mathematical model of the spine was exercised to identify mechanisms of neck injury due to hyperflexion. Loss of pilots due to ditching at sea was one of the motivations for this study. It was found that helmets have the potential of increasing injury severity particularly during a combined $+G_z$ and $-G_x$ impact, with the pulses coincident in time. The four parameters that are potentially injurious are neck shear, chin-chest contact force, odontoid process excursion into the spinal canal and spinal cord stretch.

DD FORM 1 JAN 73 1473 EDITION OF 1 NOV 65 IS OBSOLETE

SECURITY CLASSIFICATION OF THIS PAGE (When Data Entered)

411 121

SIMULATION OF HEAD AND NECK RESPONSE TO $-G_x$ AND $+G_z$ IMPACTS

by

A. I. King, S. S. Nakhla and N. K. Mital

Wayne State University
Bioengineering Center
Detroit, Michigan 48202
U.S.A.

SUMMARY

A two-dimensional mathematical model of the spine was exercised to identify mechanisms of neck injury due to hyperflexion. Loss of pilots due to ditching at sea was one of the motivations for this study. It was found that helmets have the potential of increasing injury severity particularly during a combined $+G_z$ and $-G_x$ impact, with the pulses coincident in time. The four parameters that are potentially injurious are neck shear, chin-chest contact force, odontoid process excursion into the spinal canal and spinal cord stretch.

1. INTRODUCTION

Hyperextension injuries of the neck have been extensively studied as a result of the common 'whiplash' syndrome. However, neck injuries due to head motion are not restricted to this mechanism. Ewing and Thomas (1) have conducted studies on head and neck kinematics during hyperflexion, using living human volunteers. Mertz and Patrick (2) have used both volunteers and cadavers to establish the strength and response of the human neck. They provided a response envelope for both flexion and extension. Hyperflexion injuries of the neck have been sustained by automobile crash victims involved in frontal collisions ($-G_x$ acceleration), as reported by Patrick and Andersson (3). The problem of ditching fatalities was reported by Wolff et al (4). Navy pilots who miss the carrier deck and ditch in full view of the carrier were unable to eject and were lost along with the aircraft. They were apparently concussed although there was no evidence of direct head impact with the aircraft interior. In addition, protective helmets were worn. This is a cursory review of the neck injury problem and points to the need for a deeper understanding of the mechanisms involved and the eventual establishment of a set of injury criteria for the neck.

This paper is concerned with a parametric study of neck response using a validated mathematical model of the head and spinal column developed by Tennyson and King (5). The purpose of the investigation is to quantify certain kinematic and kinetic variables which can cause injury to the central nervous system (CNS) but are not currently identifiable from experimental studies using other forms of human surrogates. One of the principal variables is the helmet which increases the mass and mass moment of inertia of the head and is not usually worn by civilians involved in automobile accidents. The effects of a combined $+G_z$ and $-G_x$ impact were analyzed using a triangular 10-g pulse for each direction of impact. The relative time of occurrence of the 2 peak acceleration was varied to demonstrate differences in response. The principal dependent variables of this study are neck shear and moment, head linear and angular acceleration and displacement, odontoid process motion into the spinal canal, stretch of the cervical cord and chin-chest contact force.

2. MATHEMATICAL MODELS OF THE SPINE

In a recent survey of mathematical models simulating impact of biomechanical systems, King and Chou (6) cited a variety of lumped and discrete parameter models as well as continuum models of the spine. Developments subsequent to this survey include the introduction of three dimensional models by Schwer (7) and the simulation of muscular response. Huston and Advani (8) proposed a head and neck model which consisted of the head, 7 cervical vertebrae and the torso. It was validated against experimental data obtained by Ewing and Thomas (1) who subjected human volunteers to $-G_x$ acceleration impacts on a horizontal sled. The correlation was very good. Muscle action was included in the model but neuromuscular delay was not properly simulated. There was no muscle force for the first 100 ms and thereafter it was an instantaneous function of stretch and stretch rate. Pontius and Liu (9) formulated a head and neck neuro-muscular model from the model by Orne and Liu (10). The muscle configuration consisted of active elements between adjacent vertebrae and there were no muscles which spanned more than one disc space. Muscle force was assumed to be function of stretch only and the delay was simulated properly by storing the stretch information for a predetermined delay period of 40 to 80 ms. There was also a muscle activation level to simulate a tensed or relaxed state. The model was exercised to simulate a mild 'whiplash' but model results were not compared with any experimental data.

Tennyson and King (5) proposed a biodynamic model of the spine to simulate the action of the spinal musculature on a discrete parameter vertebral column model conceptually similar to the one developed by Prasad and King (11). It is, thus, a two-dimensional model which can simulate motion of the head, the pelvis and the 24 vertebrae in the mid-sagittal plane. Each segment was treated as a rigid body and was assigned to carry a portion of the torso weight which was eccentric with respect to the centerline of the spine. The rigid bodies assumed a trapezoidal shape and were arranged to simulate the spinal curvatures as closely as possible. The dual load path through the spinal column was modelled by treating the intervertebral discs and posterior vertebral structure as massless deformable

elements. The disc is an elastic element capable of simultaneously resisting axial and shear loads and bending moments. The posterior vertebral structure (facets) was taken to be a spring element which could transmit axial and shear forces. Auxiliary forces were added to the appropriate vertebrae to simulate external contact forces, such as loads due to the shoulder harness, the lap belt and the seat back. It was also possible to simulate chin-chest contact.

The principal muscles represented in the model are the postero-lateral musculature of the spine. These include the deep musculature which is divided into three longitudinal muscle masses, each comprising many overlapping fascicles. The deepest and most medial muscle group is the transversospinalis system, consisting of the interspinalis, rotatores, multifidus, spinalis, semi-spinalis and semispinalis capitis. The longissimus system is lateral to the transversospinalis system and consists of overlapping fascicles extending from all the vertebrae to the head. The longissimus thoracis and lumborum are the strongest muscles of the trunk having their origin at the iliac crest of the pelvis and insertions in all the lumbar and thoracic vertebrae. The longissimus cervicis and capitas are continuations of the longissimus thoracis, having their insertions in the cervical vertebrae and on the mastoid part of the temporal bone. The illiocostalis system is lateral most with its caudal fascicles originating on the ilium and cranial fascicles extending to the seventh cervical vertebra.

The following assumptions were made in the development of muscle model:

(a) All load transmitting (passive) elements in the posterior structure of the spine including the passive component of muscle were included in the facet model. That is, in compression the 'facet' represented facet joint and spinous process interaction. In tension, the facet model simulated the action of the facet joints, spinous ligaments and passive muscle components.

(b) The active mode elements for force generators linked vertebra to vertebra posteriorly and were essentially in parallel with the facets.

(c) The muscle contractile force was taken to be a linear function of stretch and stretch rate.

(d) The transversospinalis system was represented by the active elements which linked adjacent vertebra.

(e) The longissimus and iliocostalis systems were represented by a 'linked' muscle system with an insertion at every vertebral level and the head. The contractile force was based on a summation of the activity in the individual active elements. This muscle system was anchored inferiorly in the pelvis.

(f) A numerical scheme was developed to store the activity of each contractile element for subseqent recall so that a variable neural time delay of up to 100 ms could be simulated.

(g) As the predominant passive response of the spinal column was one of flexion during $-G_x$ acceleration, only the extensor half of the spinal musculature was modelled.

(h) Muscular tetany was represented by setting a maximum allowable force developable by any particular muscle.

(i) Neural activity was confined to the 'stretch reflex' phenomenon and the γ-efferent effect remained constant.

It was shown by Tennyson and King (5) that this model simulated very well the head and neck response of a living human subject who was subjected to a $-G_x$ acceleration of 8.1 g. The data were acquired by Ewing and Thomas (1) and the input pulse was sled acceleration, necessitating the use of the entire spine in the model. In a second paper by Tennyson and King (12), it was exercised to reproduce a $-G_x$ acceleration of 5.7 g on the same subject to demonstrate its repeatability. For the same model constants and spinal geometry, the results of the model agreed well with experimental data. Due to the lack of flexors in the neck, the results are only valid for the first 240 ms during which most of the injury would have occurred. Furthermore, this model was validated against cadaveric data for $+G_z$ acceleration by Prasad and King (11), using a version with no muscular response.

This model possesses sufficient flexibility for the parametric study outlined above. The input data set was modified to accept a helmeted head and the model was used to simulate a ditching impact involving a combined $+G_z$ and $-G_x$ acceleration. The peak g-level was restricted to 10 g so as not to overwhelm completely the muscular response of the model.

The weight of the helmet was assumed to be 13.3 N (3 lb) and the combined mass moment of inertia about the lateral centroidal axis was computed to be 11.55×10^{-3} kg-m^2 (164.18 lb-s^2/in) by assuming that the helmet to be a spherical shell. The corresponding mass moment of inertia for the head above was taken to be 7.66×10^{-3} kg-m^{-2} (108.81 lb-s^2/in). The shift in the center of gravity due to the helmet was 12.7 mm anteriorly. Several runs were also made with a cephalad shift of 12.7 mm.

3. RESULTS

The input pulse for a combined $+G_z$ and $-G_x$ impact is shown in Figure 1. The simulation

started 20 ms before onset of acceleration and the peaks of the triangular pulses were assumed to occur simultaneously (Case 1) or one peak preceded the other by 50 ms, (Cases 2 and 3). The magnitude of both peaks was 10 g and the duration of each pulse was 200 ms. The rate onset was 200 g/s. The three impact conditions are identified as follows:

Case No.	Symbol	Condition
1	TOGETHER	Simultaneous $+G_z$ and $-G_x$ impact
2	Z THEN X	$+G_z$ impact occurring 50 ms before the $-G_x$ impact
3	X THEN Z	$-G_x$ impact occurring 50 ms before the $+G_z$ impact

The subject was assumed to be in a seated position restrained by a full military harness consisting of a lap belt and an inverted-Y shoulder belt. The pelvis was subjected to the impact pulse shown in Figure 1 and the resulting response of the head and neck is analyzed for possible injury mechanisms. The helmet is assumed to cause a 12.7 mm anterior shift of the head center of gravity.

Figure 2 through 4 show spinal kinematics for a helmeted head for the 3 impact conditions. They show the initial spinal shape (dotted line) and that for extreme forward flexion at the time indicated on the figure (solid line), describing qualitatively the extent of the vertical and horizontal displacement of the head as well as that of its rotation relative to T1 or the inertial reference frame. The corresponding spinal shapes for the case without a helmet are shown in Figures 5 through 7. It is seen that maximum hyperflexion is attained in Case 3, with or without a helmet.

Quantitative data are provided in terms of time history plots of the various parameters that can produce injury. A set of 8 plots for the case of simultaneous $+G_z$ and $-G_x$ peaks (Case 1) is shown in Figure 8 through 15. In each figure, the effect of the helmet is demonstrated. The peak value for disc shear at C1/C2 is doubled due to the helmet, as shown in Figure 8. There is a double contact of the chin with the chest, as shown in Figure 9. The increase in chin-chest force due to the helmet is approximately 30%. Figure 10 shows the vertical acceleration of the head relative to the inertial reference frame. The large positive values coincide with chin-chest contact and the increase in peak acceleration is also approximately 30%. In view of the fact that the helmet causes an increase in the mass moment of inertia of the head, the angular acceleration of the head is reduced when a helmet is worn. This is shown in Figure 11. The horizontal displacement of the head is not affected by the helmet as shown in Figure 12 but the vertical displacement is substantially increased as shown in Figure 13. Since the magnitude of head acceleration is relatively low, other causes of concussion are examined. Fielding (13) has stated that the motion of the odontoid process into the spinal canal is a possible cause for spinal cord injury. Figure 14 shows the extent of this excursion. It is less than 3 mm without the helmet and over 6 mm with the helmet. Another possible source of injury to the CNS is spinal cord stretch which was demonstrated in cats by Friede (14). Figure 15 compares the stretch of the cervical cord and shows a 19% increase due to the helmet. The simultaneous occurrence of the peaks for the $+G_z$ and $-G_x$ acceleration appears to cause a large percentage increase in disc shear, chin-chest contact force, vertical head acceleration, vertical head displacement odontoid process motion and spinal cord stretch. For the other two cases in which the peaks are separated by a 50-ms duration, the increase in the quantities are less pronounced or non-existent. When the $-G_x$ acceleration peak precedes that of the $+G_z$ acceleration (Case 3), there is very little change in disc shear at C1/C2 (Figure 16), chin-chest contact force (Figure 17), odontoid process motion (Figure 18) and cervical cord stretch (Figure 19). The corresponding curves for Case 2, in which the $+G_z$ acceleration pulse precedes the $-G_x$ pulse by 50 ms, are shown in Figures 20 through 23. The helmet causes a slight increase in these parameters.

The three impact cases can also be compared simultaneously. Figures 24 and 25 show cervical cord stretch for the helmeted and unhelmeted head respectively. It is most severe in Case 1 with helmet and in Case 2 without helmet. The corresponding curves for odontoid process motion are shown in Figures 26 and 27. The displacement is most pronounced for Case 1 with or without helmet.

Table 1 summarizes the peak values of 11 parameters for all 3 impact cases, with and without helmet. The disc and facet shear force are at the level of C1/C2. The rotation of the head is with respect to T1 and the negative sign represents a relative clockwise rotation. All maximum values given in this table occurred at or before 240 ms of simulation.

If the combined center of gravity of the head and helmet was assumed to be shifted caudally by 12.7 mm, the change in injury parameters was surprisingly less severe, as shown in Table 2. For Case 1, there was an increase in head rotation with respect to T1 in comparison with the coresponding value for an anterior shift in the center of gravity. Head displacement also increased but all other values were lower. In the other 2 cases, there was also more head rotation but the other parameters were not altered significantly in comparison with the corresponding values in Table 1. For the helmeted head, conditions are generally most severe for Case 1 when the 2 pulses are coincident. However, the chin-chest contact force is highest in Case 2 and spinal cord stretch is the largest in Case 3.

4. DISCUSSION AND CONCLUSIONS

Spinal cord injury has been identified as a possible cause of concussion when there is no direct head impact. The involvement of the CNS precludes the use of human volunteers or cadaveric subjects. Anthropomorphic and species differences render the results of animal testing somewhat uncertain. An attempt has been made to demonstrate possible mechanisms of

injury using the mathematical model as a human surrogate. The model has been validated against human volunteer and cadaveric data and is expected to yield reasonable results. However, its results are always subject to experimental verification.

A comparison of 3 impact cases with and without helmet was made using a 2-dimensional model of the spine. The same model constants were used for all runs and changes in response could be considered as more reliable than absolute values. The combined $+G_z$ and $-G_x$ impact acceleration pulse was used primarily to simulate a ditching at sea, during which it is possible to have the pulses occur simultaneously or one before the other. A hypothetical profile was selected and a rather low peak acceleration was assumed so as not to overwhelm completely all passive muscular response.

In general, the helmet increased the disc and facet shear forces, resulting in an increased displacement of the odontoid process into the spinal canal. There was also a general increase in spinal cord stretch, chin-chest contact force and head displacement. Head angular acceleration showed a significant decrease. Conditions were most severe when the $+G_z$ and $-G_x$ pulses coincided in time and when the helmet was worn. Spinal cord stretch was over 40 mm with or without helmet for Case 3, in which the $-G_x$ pulse preceded the $+G_z$ pulse. The corresponding values for Case 2 were much lower.

An anterior shift of 12.7 mm in the center of gravity due to the helmet is apparently less desirable than a cephalad shift of the same magnitude. There was less stretch in the cervical cord and the maximum displacement of the odontoid process was approximately the same for all 3 cases with helmet.

In conclusion, this parametric study has identified some possible mechanisms of injury to the cord during hyperflexion of the neck. It has also facilitated future experimental studies by pointing out the conditions that are likely to be most hazardous. The helmet has the potential of increasing injury severity, particularly when the two pulses are coincident in time. The four parameters which are potentially injurious are neck shear, chin-chest contact force, displacement of the odontoid process and spinal cord stretch. They are of higher magnitude for an anterior shift of the head center of gravity in comparison with a cephalad shift of the same magnitude (12.7 mm). This result contradicts intuition and should be verified experimentally.

5. REFERENCES

1. Ewing, C.L. and Thomas, D.J., "Human Head and Neck Response to Impact Acceleration," Naval Aerospace Medical Research Laboratory, NAMRL Monograph 21, August, 1972.

2. Mertz, H.J. and Patrick, L.M., "Strength and Response of the Human Neck," Proc. 15th Stapp Car Crash Conference, SAE, Warrendale, SAE Paper No. 710855, pp. 207-255, 1971

3. Patrick, L.M. and Andersson, A., "Three-Point Harness Accident and Laboratory Data Comparison," Proc. 18th Stapp Car Crash Conference, SAE Warrendale, SAE Paper No. 741181, pp 201-282, 1974.

4. Wolff, J. et al, "Development of a Method for Evaluating Means for Reducing Impact Injuries to Pilots in Aircraft Accidents, "Technical Report No. 69-68-7, Final Report by Serendipity Associates, 1968.

5. Tennyson, S.A. and King, A.I., "A Biodynamic Model of the Human Spinal Column," SAE Transactions, pp 2430-2443, 1976.

6. King, A.I. and Chou, C.C., "Mathematical Modelling, Simulation and Experimental Testing of Biomechanical System Crash Response". J. of Biomech. Vol 9, pp 301-318, 1976.

7. Schwer, L.E., "A Three-Dimensional Large Displacement Transient Analysis of the Human Spine and Torso," Ph.D. Thesis, University of Illinois, Chicago, 1976.

8. Huston, J.C. and Advani, S.H., "Three-Dimensional Model of the Human Head and Neck for Automobile Biodynamic Response to Impact", in Mathematical Modeling Biodynamic Response to Impact, SAE Publication No. SP-412, pp 9-20, 1976.

9. Pontius, U.R. and Liu, Y.K., "Neuromuscular Cervical Spine Model for Whiplash", in Mathematical Modeling Biodynamic Response to Impact, SAE Publication No. SP-412, pp 21-30, 1976

10. Orne, D. and Liu, Y.K., "Mathematical Model of Spinal Response to Impact". J. of Biomech., Vol. 4, pp 49-72, 1970.

11. Prasad, P. and King, A.I., "An Experimentally Validated Dynamic Model of the Spine, J. of Appl. Mech., Vol. 41, pp 546-550, 1974.

12. Tennyson, S.A. and King, A.I., "Mathematical Models of the Spine," Proc. 1st International Conf. on Mathematical Modeling, Ed. by X.J.R. Avula, U. of Missouri-Rolla, Vol. II, pp 977-985, 1977.

13. Fielding, W., Recorded Statement made at Head and Neck Injury Workshop sponsored by the National Motor Vehicle Safety Council, held in Washington, D.C., 1977.

14. Friede, R.L., "Specific Cord Damage at the Atlas Level as a Pathogenic Mechanism in Cerebral Concussion," J. of Neuropathology and Experimental Neurology, Vol. 19, pp 266-279, 1960.

6. ACKNOWLEDGMENT

This research was supported in part by ONR Contract No. N00014-75-C-1015.

Table 1 - Summary of Peak Values For Anterior Shift of C. G.

Case No. / Symbol / Parameter	1 TOGETHER W/O Helmet	1 TOGETHER W/Helmet	2 Z THEN X W/O Helmet	2 Z THEN X W/Helmet	3 X THEN Z W/O Helmet	3 X THEN Z W/Helmet
Disc. Shear @C1/C2 (N)	399	868	358	409	234	262
Facet Shear @C1/C2 (N)	361	814	357	424	226	260
Chin-Chest Force (n)	2733	3534	3533	3795	3315	3437
Head Vert. Accel (g)	44.5	58.4	57.4	40.6	56.3	48.3
Head Horiz. Accel (g)	45.8	37.4	33.5	33.1	27.1	16.3
Head Ang. Accel (Rad/s^2)	5267	3922	5369	4745	4538	3236
Head Horiz. Disp. (mm)	201	208	185	190	209	211
Head Vert. Disp. (mm)	172	191	200	192	186	187
Odontoid Disp. (mm)	2.9	6.2	2.6	3.1	1.8	2.0
Cord Stretch (mm)	36.4	43.3	29.4	33.4	41.0	40.6
Head Rot. (deg) (with respect to T1)	-77.5	-73.4	-68.9	-65.6	-69.1	-65.0

Table 2 - Summary of Peak Values For Caudal Shift of C. G.

Case No. / Symbol / Parameter	1 TOGETHER W/O Helmet	1 TOGETHER W/Helmet	2 Z THEN X W/O Helmet	2 Z THEN X W/Helmet	3 X THEN Z W/O Helmet	3 X THEN Z W/Helmet
Disc. Shear @C1/C2 (N)	399	854	358	527	234	249
Facet Shear @C1/C2 (N)	361	797	357	486	226	245
Chin-Chest Force (n)	2733	2881	3533	3874	3315	3079
Head Vert. Accel (g)	44.5	51.2	57.4	40.2	56.3	46.2
Head Horiz. Accel (g)	45.8	42.4	33.5	40.8	27.1	15.7
Head Ang. Accel (Rad/s^2)	5267	3653	5369	3905	4538	3022
Head Horiz. Disp. (mm)	201	216	185	202	209	221
Head Vert. Disp. (mm)	172	209	200	171	186	201
Odontoid Disp. (mm)	2.9	5.2	2.6	3.8	1.8	2.3
Cord Stretch (mm)	36.4	38.2	29.4	28.6	41.0	39.4
Head Rot. (deg) (with respect to T1)	-77.5	-83.6	-68.9	-74.3	-69.1	-77.7

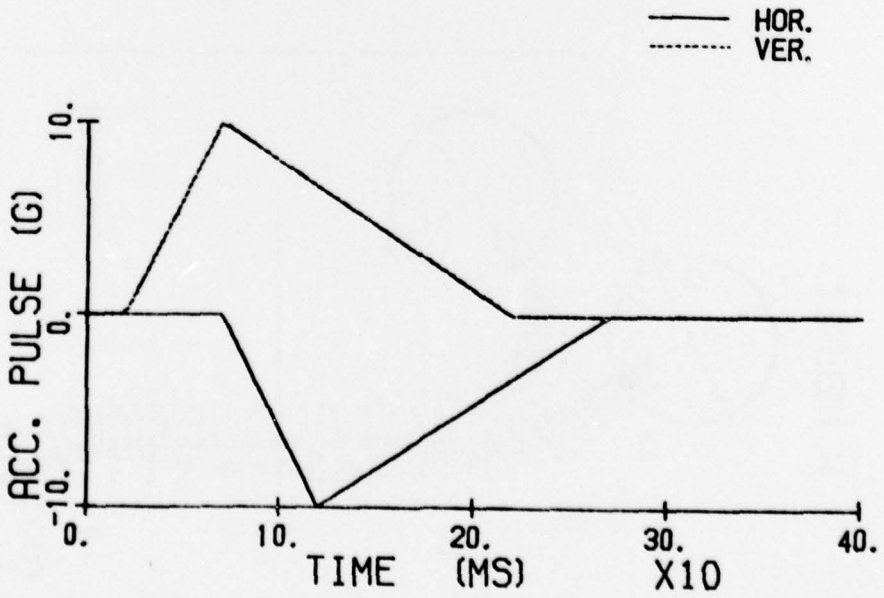

Fig. 1 Combined $+G_z$ and $-G_x$ Input Pulses (Case 2 shown)

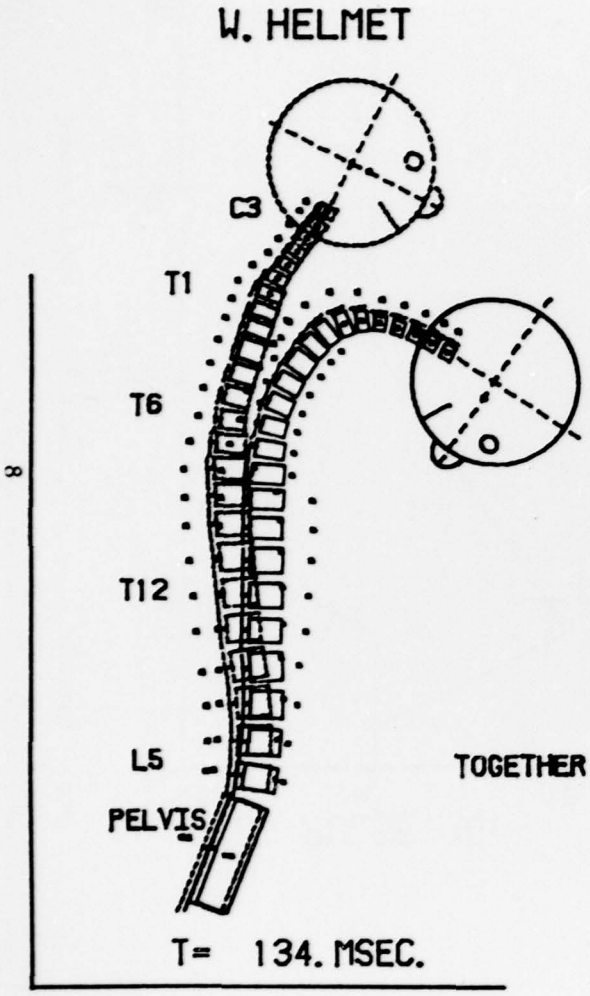

Fig.2 Spinal Kinematics with Helmet, Case 1

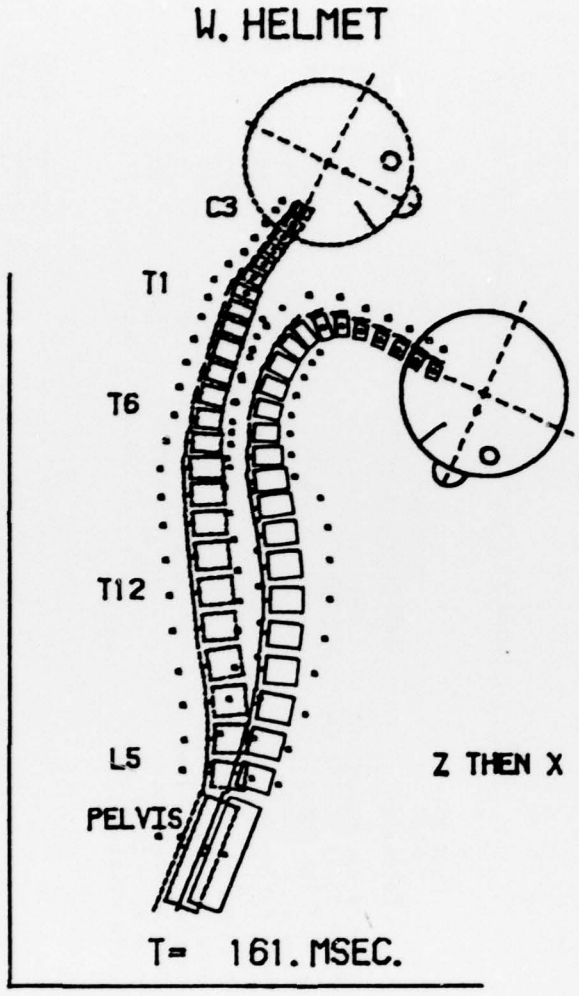

Fig.3 Spinal Kinematics with Helmet, Case 2

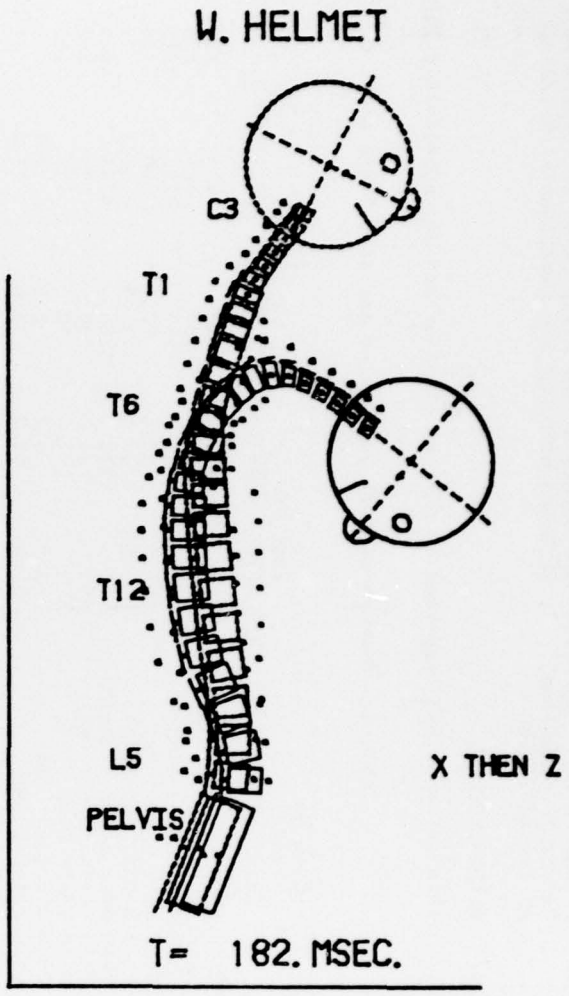

Fig.4 Spinal Kinematics with Helmet, Case 3

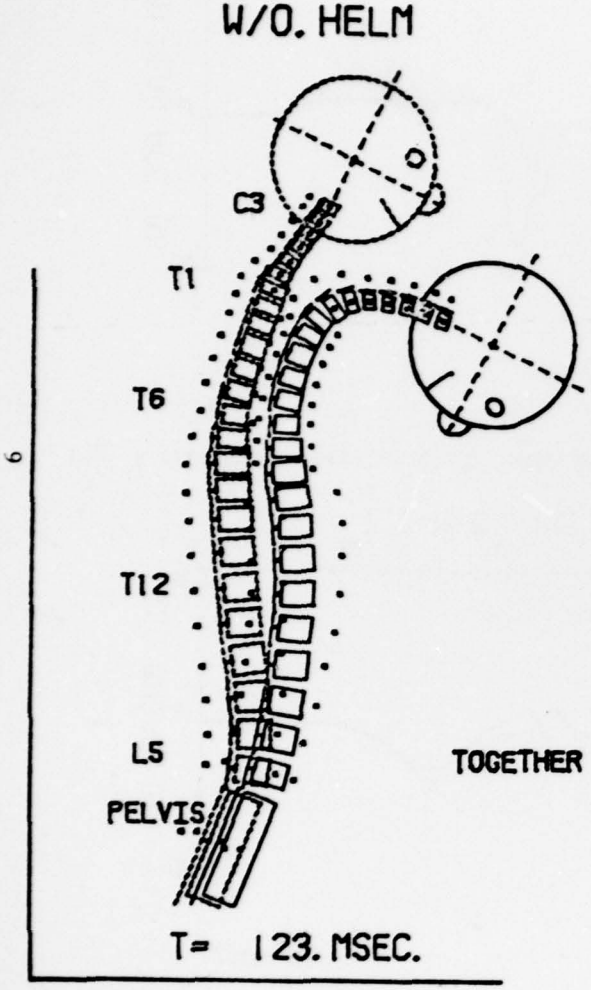

Fig.5 Spinal Kinematics Without Helmet, Case 1

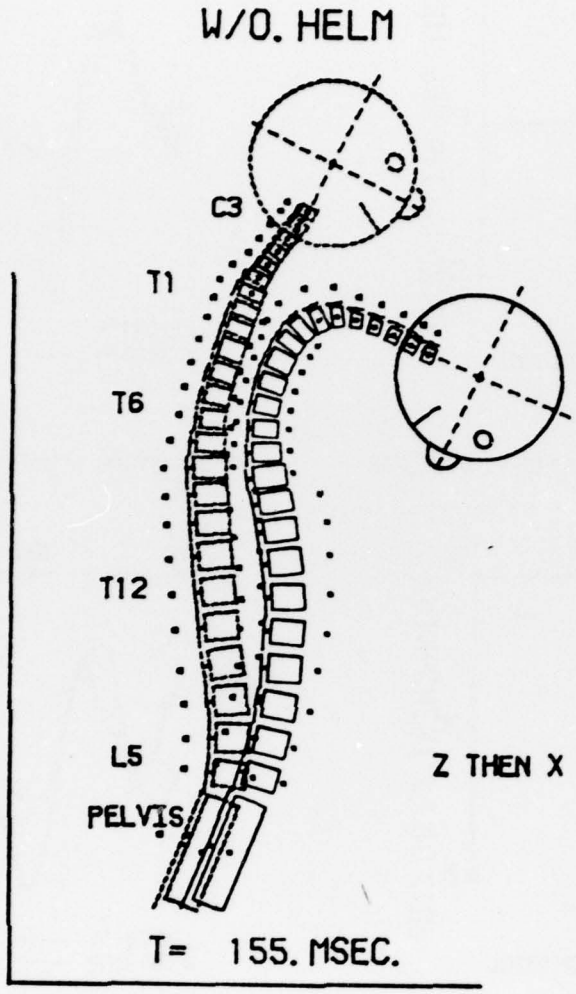

Fig.6 Spinal Kinematics Without Helmet, Case 2

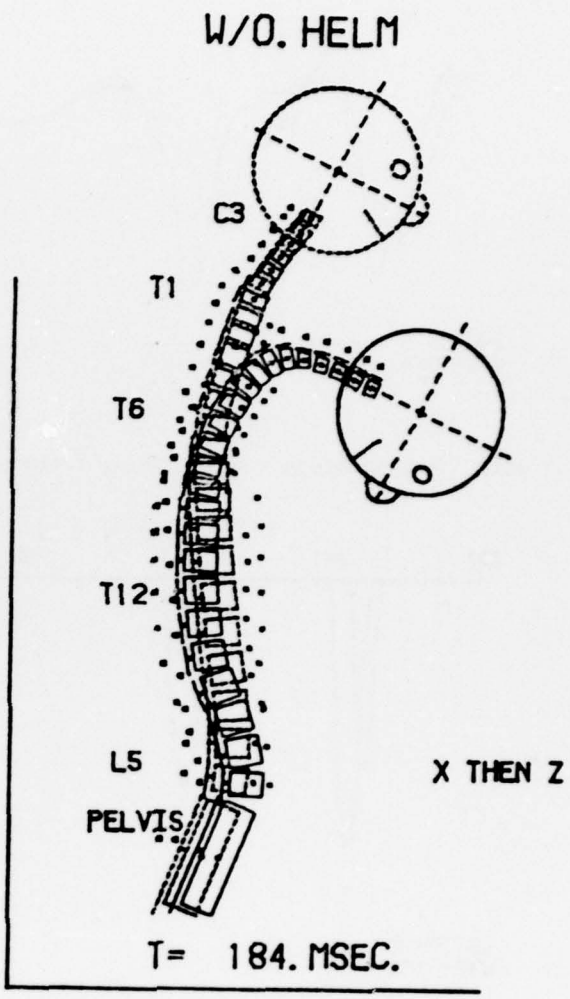

Fig.7 Spinal Kinematics Without Helmet

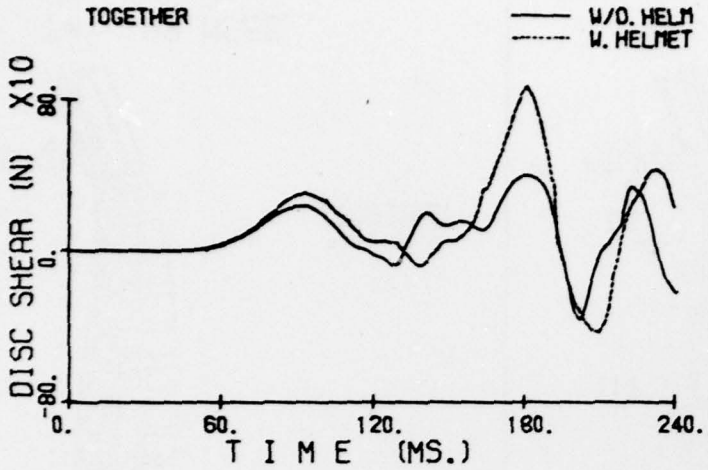

Fig. 8 Disc Shear Force at C1/C2, with and without Helmet, Case 1

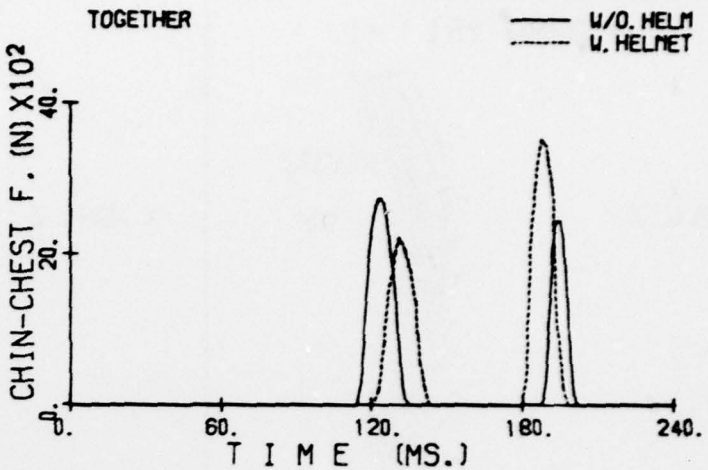

Fig. 9 Chin-Chest Contact Force, with & WithoutHelmet, Case 1

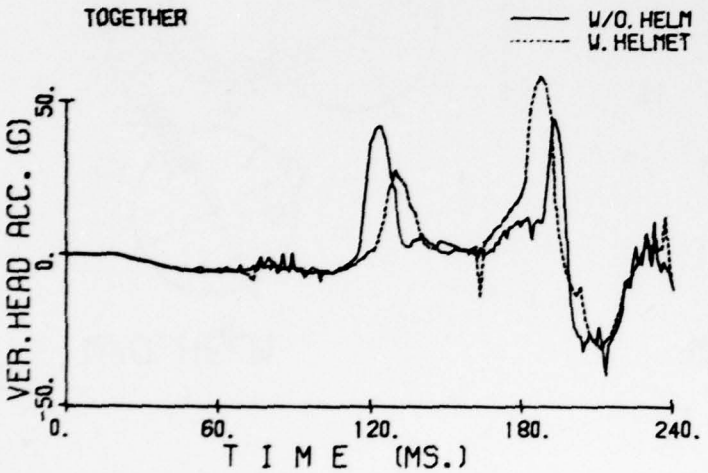

Fig. 10 Vertical Acceleration of the Head, with & Without Helmet, Case 1

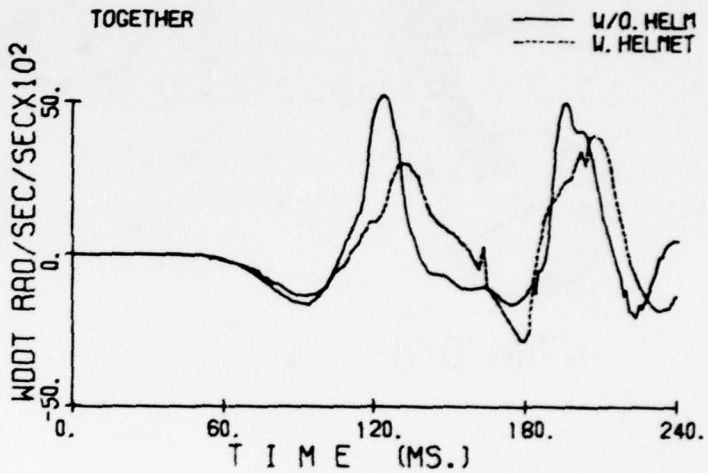

Fig. 11 Angular Acceleration of the Head, with & Without Helmet, Case 1

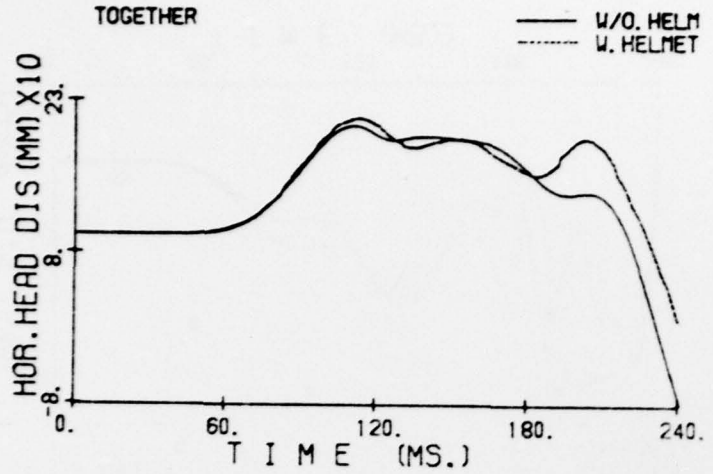

Fig. 12 Horizontal Displacement of the Head, with & without Helmet, Case 1

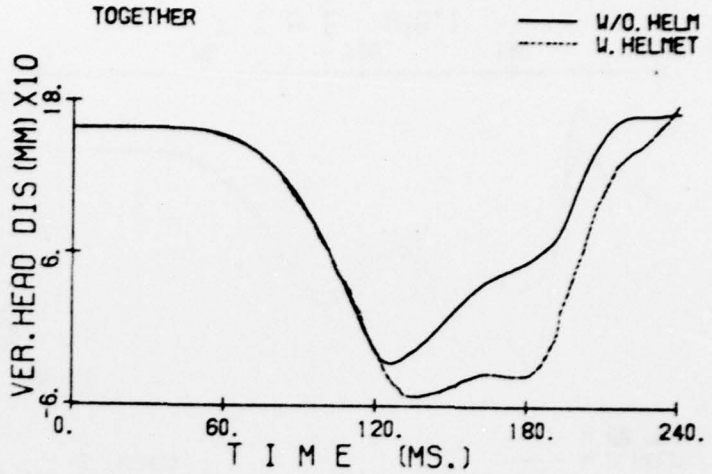

Fig. 13 Vertical Displacement of the Head, with & without Helmet, Case 1

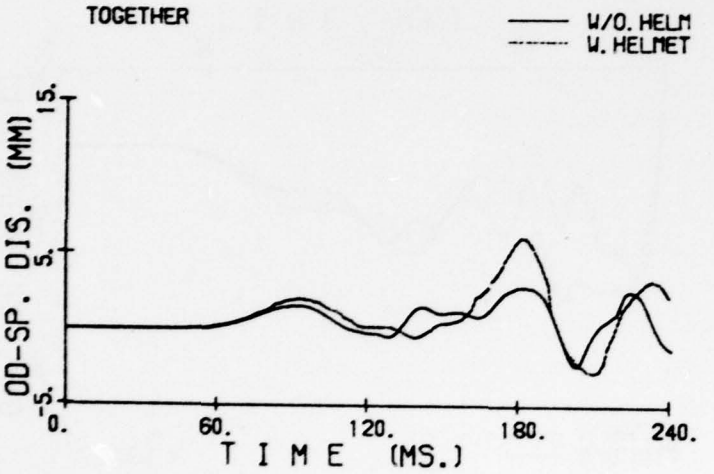

Fig. 14 Odontoid Process Displacement into the Spinal Canal, with & without Helmet, Case 1

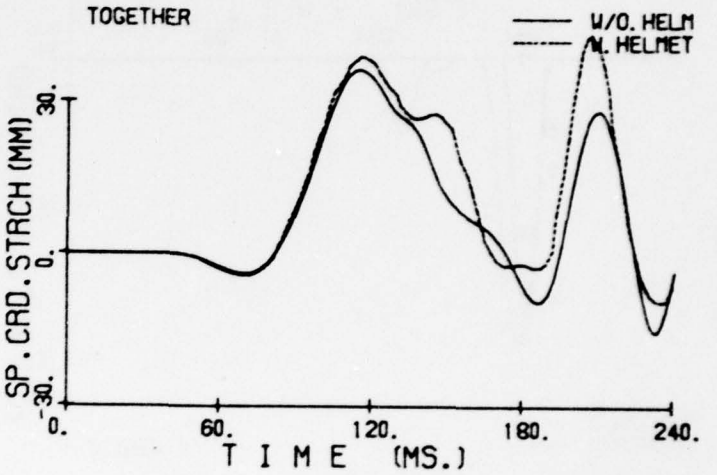

Fig. 15 Spinal Cord Stretch, with & without Helmet, Case 1

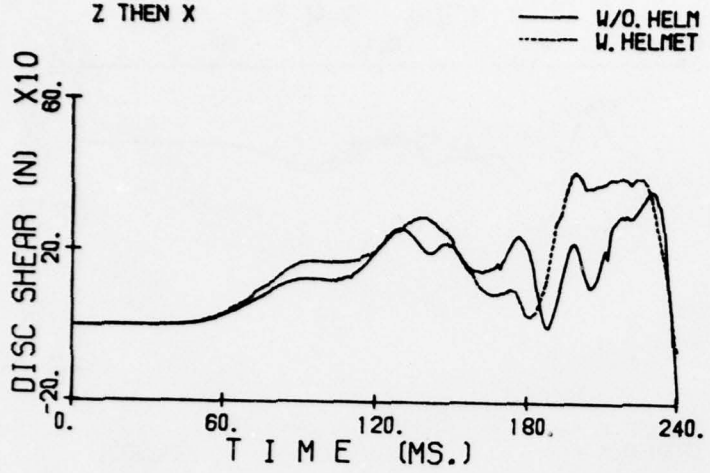

Fig. 16 Disc Shear Force at C1/C2, with & without Helmet, Case 2

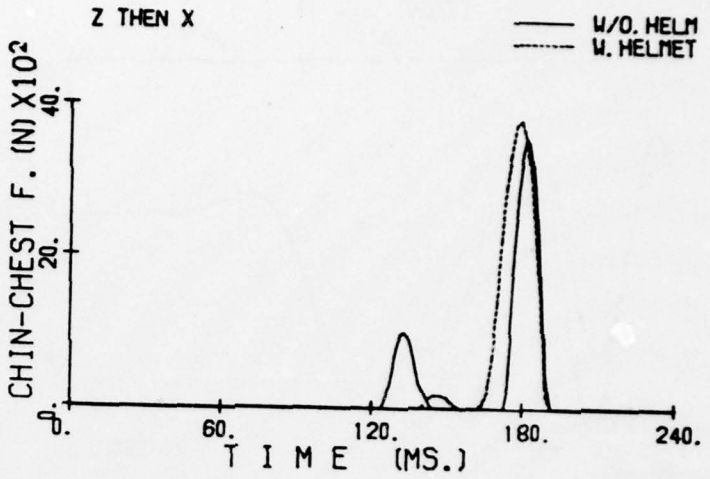

Fig. 17 Chin-Chest Contact Force, with & without Helmet, Case 2

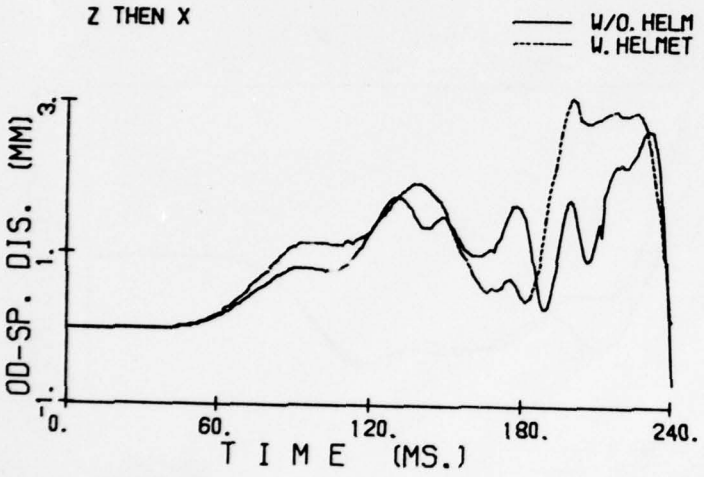

Fig. 18 Odontoid Process Displacement into the Spinal Canal with & without Helmet, Case 2

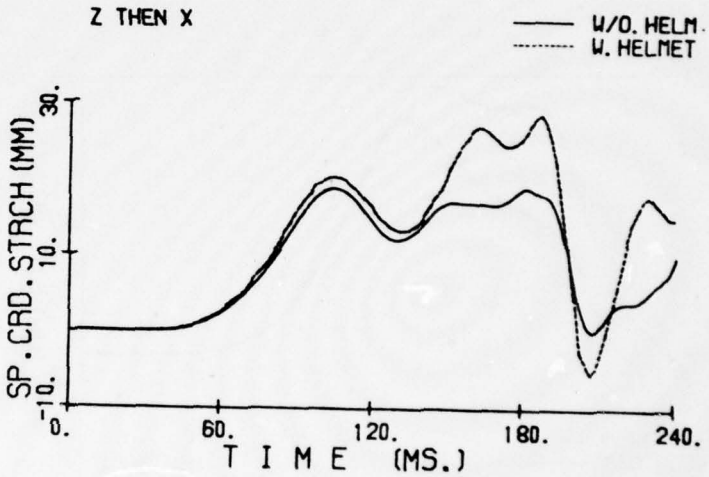

Fig. 19 Spinal Cord Stretch, with & without Helmet, Case 2

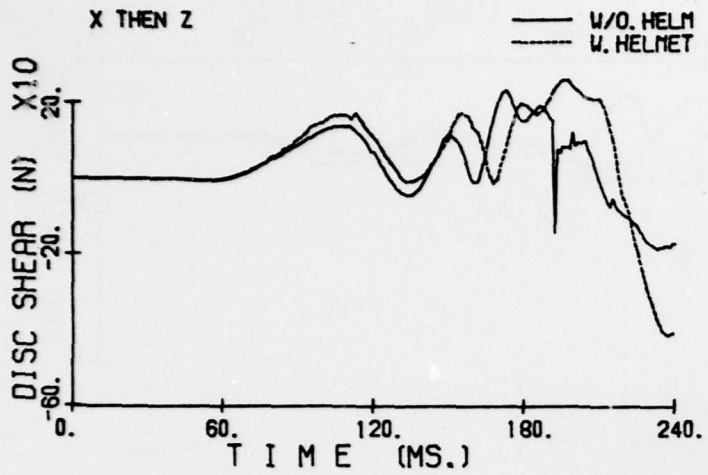

Fig. 20 Disc Shear Force at C1/C2, with & without Helmet, Case 3

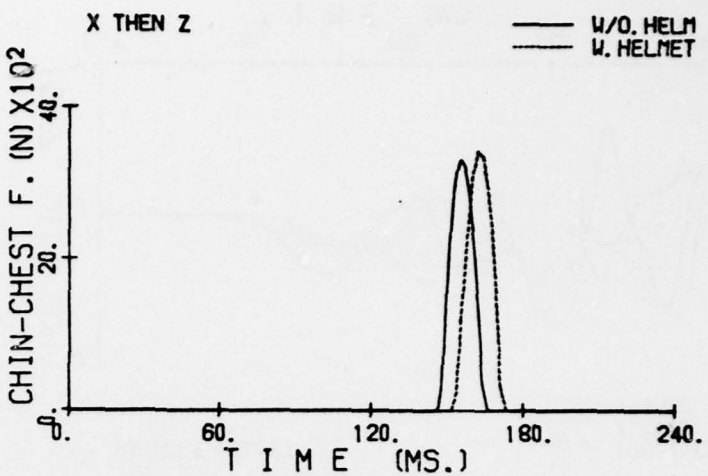

Fig. 21 Chin-Chest Contact Force, with 7 without Helmet, Case 3

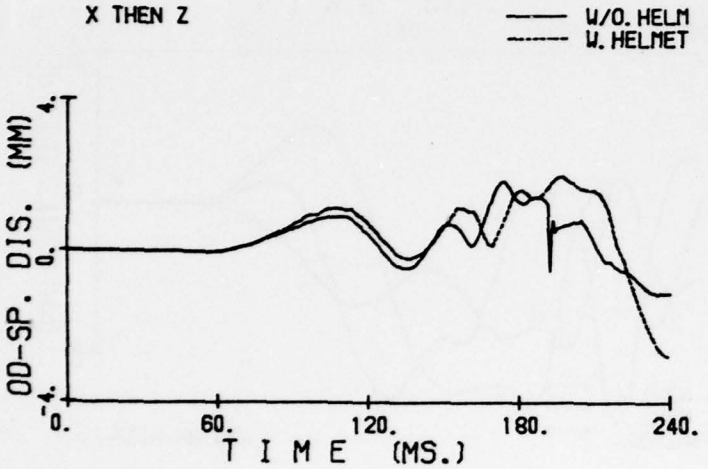

Fig. 22 Odontoid Process Displacement into the Spinal Canal, with & without Helmet, Case 3

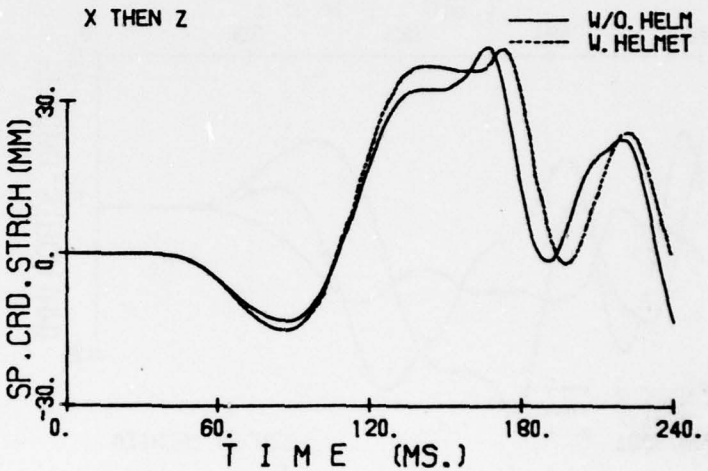

Fig. 23 Spinal Cord Stretch, with & without Helmet, Case 3

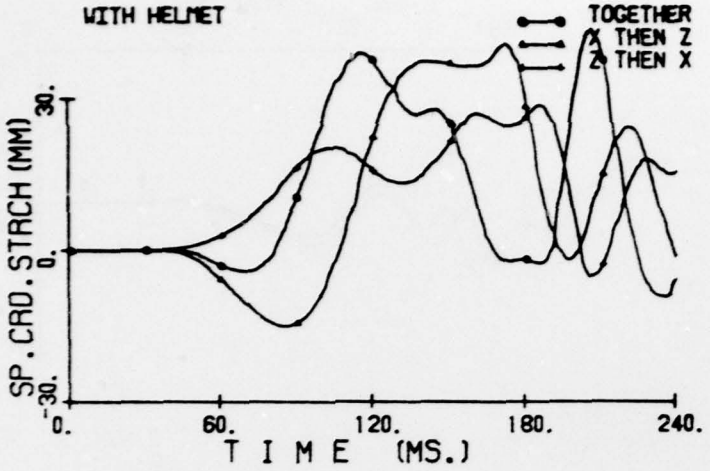

Fig. 24 Spinal Cord Stretch with Helmet, Cases 1 through 3

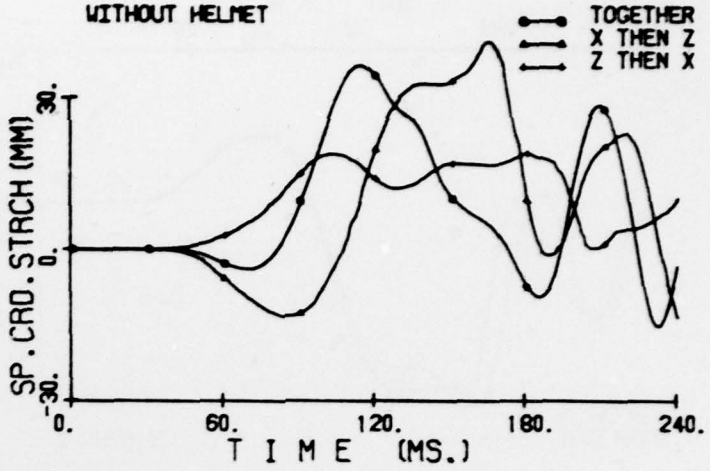

Fig. 25 Spinal Cord Stretch without Helmet, Cases 1 through 3

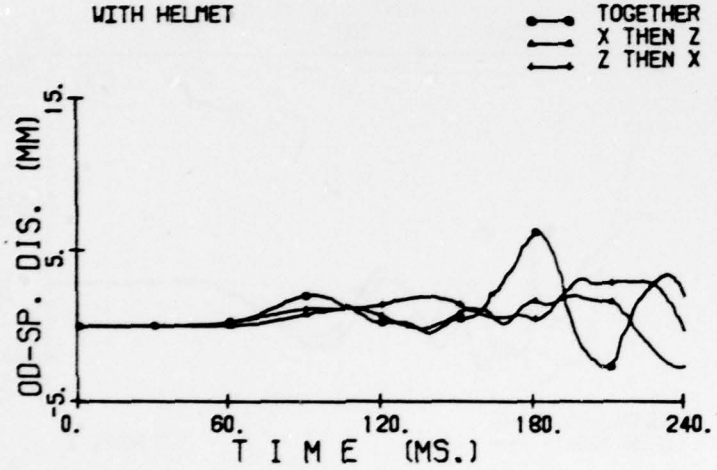

Fig. 26 Odontoid Process Displacement into the Spinal Canal with Helmet, Cases 1 through 3

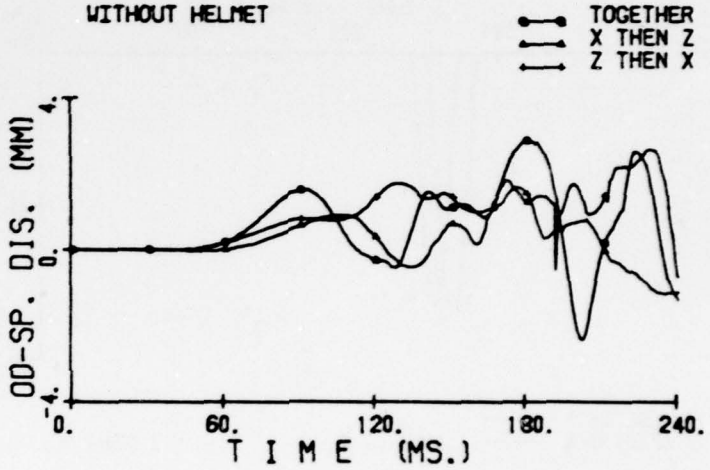

Fig. 27 Odontoid Process Displacement into the Spinal Canal without Helmet, Cases 1 through 3

PART 1 - GOVERNMENT

Administrative & Liaison Activities

Chief of Naval Research
Department of the Navy
Arlington, Virginia 22217
  Attn: Code 474 (2)
        471
        222

Director
ONR Branch Office
495 Summer Street
Boston, Massachusetts 02210

Director
ONR Branch Office
219 S. Dearborn Street
Chicago, Illinois 60604

Director
Naval Research Laboratory
Attn: Code 2629 (ONRL)
Washington, D.C. 20390 (6)

U.S. Naval Research Laboratory
Attn: Code 2627
Washington, D.C. 20390

Director
ONR - New York Area Office
715 Broadway - 5th Floor
New York, N.Y. 10003

Director
ONR Branch Office
1030 E. Green Street
Pasadena, California 91101

Defense Documentation Center
Cameron Station
Alexandria, Virginia 22314 (12)

Army

Commanding Officer
U.S. Army Research Office Durham
Attn: Mr. J. J. Murray
CRD-AA-IP
Box CM, Duke Station
Durham, North Carolina 27706 (2)

Commanding Officer
AMXMR-ATL
Attn: Mr. B. Shea
US Army Materials Res. Agency
Watertown, Massachusetts 02172

Watervliet Arsenal
Weapons Research Center
Watervliet, New York 12189
  Attn: Director of Research

Technical Library

Redstone Scientific Info. Center
Chief, Document Section
U.S. Army Missile Command
Redstone Arsenal, Alabama 35809

Army R&D Center
Fort Belvoir, Virginia 22060

Navy

Commanding Officer and Director
Naval Ship Research & Development Center
Bethesda, Maryland 20034
  Attn: Code 042 (Tech. Lib. Br.)
        17 (Struc. Mech. Lab.)
        172
        174
        177
        1800 (Appl. Math. Lab.)
        50128 (Dr. W.D. Sette)
        18 (Dr. M.M. Sevik)
        1901 (Dr. M. Strassberg)
        1945
        196
        1962 (Dr. B. Pate)

Naval Weapons Laboratory
Dahlgren, Virginia 22448

Naval Research Laboratory
Washington, D.C. 20375
  Attn: Code 8400
        8410
        8430
        8440
        8300
        6190
        6180

Anderson Explosion Research Div.
Naval Ship R&D Center
Norfolk Naval Shipyard
Portsmouth, Virginia 23709
  Attn: Dr. B. Palmer
        Code 780

Naval Ship Research & Development Center
Annapolis Division
Annapolis, Maryland 21402
  Attn: Code 2740 - Dr. T.F. Wang
        28 - Mr. B.J. Wolfe
        281 - Mr. B.B. Biederberger
        2814 - Dr. H. Vanderveldt

Technical Library
Naval Undersea Weapons Center
Pasadena Annex
3202 E. Foothill Blvd.
Pasadena, California 91107

U.S. Naval Weapons Center
China Lake, California 93555
  Attn: Code 4062 - Mr. W. Warbeck
        4526 - Mr. Sam Stechel

Commanding Officer
U.S. Naval Civil Engr. Lab
Code L31
Port Hueneme, California 93041

Technical Director
U.S. Naval Ordnance Laboratory
White Oak
Silver Spring, Maryland 20910

Technical Director
Naval Undersea R&D Center
San Diego, California 92132

Supervisor of Shipbuilding
U.S. Navy
Newport News, Virginia 23607

Technical Director
Mare Island Naval Shipyard
Vallejo, California 94592

U.S. Navy Underwater Sound Ref. Lab.
Office of Naval Research
PO Box 8337
Orlando, Florida 32806

Chief of Naval Operations
Dept. of the Navy
Washington, D.C. 20350
  Attn: Code Op07T

Strategic Systems Project Office
Department of the Navy
Washington, D.C. 20390
  Attn: NSP-001 Chief Scientist

Deep Submergence Systems
Naval Ship Systems Command
Code 19522
Department of the Navy
Washington, D.C. 20360

Engineering Dept.
US Naval Academy
Annapolis, Maryland 21402

Naval Air Systems Command
Dept. of the Navy
Washington, D.C. 20360
  Attn: NAVAIR 5302 Aero & Structures
        5308 Structures
        520312 Materials
        604 Tech. Library
        1208 Structures

Director, Aero Mechanics
Naval Air Development Center
Johnsville
Warminster, Pennsylvania 18974

Technical Director
U.S. Naval Undersea R&D Center
San Diego, California 92132

Engineering Department
U.S. Naval Academy
Annapolis, Maryland 21402

Naval Facilities Engineering Command
Dept. of the Navy
Washington, D.C. 20360
  Attn: NAVFAC 03 Research & Development
        04 " "
        14414 Tech. Library

Naval Sea Systems Command
Dept. of the Navy
Washington, D.C. 20360
  Attn: NAVSHIP 03 Res. & Technology
        031 Ch. Scientist for R&D
        03412 Hydromechanics
        037 Ship Silencing Div.
        039 Weapons Dynamics

Naval Ship Engineering Center
Prince Georges' Plaza
Hyattsville, Maryland 20782
  Attn: NAVSEC 6100 Ship Sys. Engr. & Des. Dept.
        6102C Computer-Aided Ship Des.
        6105G
        6110 Ship Concept Design
        6120 Hull Div.
        6120D Hull Div.
        6128 Surface Ship Struct.
        6129 Submarine Struct.

Air Force

Commander WADD
Wright-Patterson Air Force Base
Dayton, Ohio 45433
  Attn: Code WWRMDD
        AFFDL (FDDS)
        Structures Division
        AFLC (MCEEA)

Chief, Applied Mechanics Group
U.S. Air Force Inst. of Tech.
Wright-Patterson Air Force Base
Dayton, Ohio 45433

Chief, Civil Engineering Branch
WLRC, Research Division
Air Force Weapons Laboratory
Kirtland AFB, New Mexico 87117

Air Force Office of Scientific Research
1400 Wilson Blvd.
Arlington, Virginia 22209
  Attn: Mechanics Div.

NASA

Structures Research Division
National Aeronautics & Space Admin.
Langley Research Center
Langley Station
Hampton, Virginia 23365

National Aeronautic & Space Admin.
Associate Administrator for Advanced
  Research & Technology
Washington, D.C. 02546

Scientific & Tech. Info. Facility
NASA Representative (S-AK/DL)
P.O. Box 5700
Bethesda, Maryland 20014

Other Government Activities

Commandant
Chief, Testing & Development Div.
U.S. Coast Guard
1300 E. Street N.W.
Washington, D.C. 20226

Technical Director
Marine Corps Dev. & Educ. Command
Quantico, Virginia 22134

Director
National Bureau of Standards
Washington, D.C. 20234
  Attn: Mr. R.L. Wilson, EM 219

Dr. M. Gaus
National Science Foundation
Engineering Division
Washington, D.C. 20550

Science & Tech. Division
Library of Congress
Washington, D.C. 20540

Director
Defense Nuclear Agency
Washington, D.C. 20305
  Attn: SPSS

Commander Field Command
Defense Nuclear Agency
Sandia Base
Albuquerque, New Mexico 87115

Director Defense Research & Engrg.
Technical Library
Room 3C-128
The Pentagon
Washington, D.C. 20301

Chief, Airframe & Equipment Branch
FS-120
Office of Flight Standards
Federal Aviation Agency
Washington, D.C. 20553

Chief, Research and Development
Maritime Administration
Washington, D.C. 20235

Deputy Chief, Office of Ship Construction
Maritime Administration
Washington, D.C. 20235
  Attn: Mr. C.E. Rieser

Atomic Energy Commission
Div. of Reactor Devel. & Tech.
Germantown, Maryland 20767

Ship Hull Research Committee
National Research Council
National Academy of Sciences
2101 Constitution Avenue
Washington, D.C. 20418
  Attn: Mr. A.R. Lytle

PART 2 - CONTRACTORS AND OTHER TECHNICAL COLLABORATORS

Universities

Dr. J. Tinsley Oden
University of Texas at Austin
341 Eng. Science Bldg.
Austin, Texas 78712

Prof. Julius Miklowitz
California Institute of Technology
Div. of Engineering & Applied Sciences
Pasadena, California 91109

Dr. Harold Liebowitz, Dean
School of Engr. & Applied Science
George Washington University
725 23rd St. N.W.
Washington, D.C. 20006

Prof. Eli Sternberg
California Institute of Technology
Div. of Engr. & Applied Sciences
Pasadena, California 91109

Prof. Paul M. Naghdi
University of California
Div. of Applied Mechanics
Etcheverry Hall
Berkeley, California 94720

Professor P.S. Symonds
Brown University
Division of Engineering
Providence, R.I. 02912

Prof. A.J. Durelli
The Catholic University of America
Civil/Mechanical Engineering
Washington, D.C. 20017

Prof. S.S. Tezcan
Columbia University
Dept. of Civil Engineering
S.W. Mudd Bldg.
New York, N.Y. 10027

Prof. H.H. Bleich
Columbia University
Dept. of Civil Engineering
Amsterdam & 120th St.
New York, N.Y. 10027

Prof. F.L. DiMaggio
Columbia University
Dept. of Civil Engineering
616 Mudd Building
New York, N.Y. 10027

Prof. [illegible]N. Freudenthal
George Washington University
School of Engineering & Applied Science
Washington, D.C. 20006

D.C. Evans
University of Utah
Computer Science Division
Salt Lake City, Utah 84112

Prof. Norman Jones
Massachusetts Inst. of Technology
Dept. of Naval Architecture & Marine Engr
Cambridge, Massachusetts 02139

Professor Albert I. King
Biomechanics Research Center
Wayne State University
Detroit, Michigan 48202

Dr. V.H. Neff, Jr.
Wayne State University
School of Medicine
Detroit, Michigan 48202

Dean B.A. Boley
Northwestern University
Technological Institute
2145 Sheridan Road
Evanston, Illinois 60201

Prof. P.G. Hodge, Jr.
University of Minnesota
Dept. of Aeronautic Engr. & Mechanics
Minneapolis, Minnesota 55455

Dr. D.C. Drucker
University of Illinois
Dean of Engineering
Urbana, Illinois 61801

Prof. N.M. Newmark
University of Illinois
Dept. of Civil Engineering
Urbana, Illinois 61801

Prof. E. Reissner
University of California, San Diego
Dept. of Applied Mechanics
La Jolla, California 92037

Prof. William A. Nash
University of Massachusetts
Dept. of Mechanics & Aerospace Engr.
Amherst, Massachusetts 01002

Library (Code 0384)
U.S. Naval Postgraduate School
Monterey, California 93940

Prof. Arnold Allentuch
Newark College of Engineering
Dept. of Mechanical Engineering
323 High Street
Newark, New Jersey 07102

Dr. George Herrmann
Stanford University
Dept. of Applied Mechanics
Stanford, California 94305

Prof. J.D. Achenbach
Northwestern University
Dept. of Civil Engineering
Evanston, Illinois 60201

Director, Applied Research Lab
Pennsylvania State University
P.O. Box 30
State College, Pennsylvania 16801

Prof. Eugen J. Skudrzyk
Pennsylvania State University
Applied Research Laboratory
Dept. of Physics - P.O. Box 30
State College, Pennsylvania 16801

Prof. J. Kempner
Polytechnic Institute of Brooklyn
Dept. of Aero. Engr. & Applied Mech.
333 Jay Street
Brooklyn, N.Y. 11201

Prof. J. Klosner
Polytechnic Institute of Brooklyn
Dept. of Aerospace & Appl. Mech.
333 Jay Street
Brooklyn, N.Y. 11201

Prof. R.A. Schapery
Texas A&M University
Dept. of Civil Engineering
College Station, Texas 77840

Prof. W.D. Pilkey
University of Virginia
Dept. of Aerospace Engineering
Charlottesville, Virginia 22903

Dr. E.C. Schaeffer
University of Maryland
Aerospace Engineering Dept.
College Park, Maryland 20742

Prof. E.D. Williams
Clarkson College of Technology
Dept. of Mechanical Engineering
Potsdam, N.Y. 13676

Dr. J.A. Strickiin
Texas A&M University
Aerospace Engineering Dept.
College Station, Texas 77843

Dr. L.A. Schmit
University of California, LA
School of Engineering & Applied Science
Los Angeles, California 90024

Dr. E.A. Kamel
The University of Arizona
Aerospace & Mech. Engineering Dept.
Tucson, Arizona 85721

Dr. B.S. Berger
University of Maryland
Dept. of Mechanical Engineering
College Park, Maryland 20742

Prof. G.R. Irwin
Dept. of Mechanical Engineering
University of Maryland
College Park, Maryland 20742

Dr. S.J. Fenves
Carnegie-Mellon University
Dept. of Civil Engineering
Schenley Park
Pittsburgh, Pennsylvania 15213

Dr. Ronald L. Huston
Dept. of Engineering Analysis
Mail Box 112
University of Cincinnati
Cincinnati, Ohio 45221

Prof. George Sih
Dept. of Mechanics
Lehigh University
Bethlehem, Pennsylvania 18015

Prof. A.S. Kobayashi
University of Washington
Dept. of Mechanical Engineering
Seattle, Washington 98195

Librarian
Webb Institute of Naval Architecture
Crescent Beach Road, Glen Cove
Long Island, New York 11542

Prof. Daniel Frederick
Virginia Polytechnic Institute
Dept. of Engineering Mechanics
Blacksburg, Virginia 24061

Prof. A.C. Eringen
Dept. of Aerospace & Mech. Sciences
Princeton University
Princeton, New Jersey 08540

Dr. S.L. Koh
School of Aero., Astro. & Engr. Sci.
Purdue University
Lafayette, Indiana

Prof. E.H. Lee
Div. of Engr. Mechanics
Stanford University
Stanford, California 94305

Prof. R.D. Mindlin
Dept. of Civil Engineering
Columbia University
S.W. Mudd Building
New York, N.Y. 10027

Prof. S.S. Dong
University of California
Dept. of Mechanics
Los Angeles, California 90024

Prof. Burt Paul
University of Pennsylvania
Towne School of Civil & Mech. Engr.
Rm. 111 - Towne Building
220 S. 33rd Street
Philadelphia, Pennsylvania 19104

Prof. H.W. Liu
Dept. of Chemical Engineering & Metall.
Syracuse University
Syracuse, N.Y. 13210

Prof. S. Bodner
Technion R&D Foundation
Haifa, Israel

Prof. E.J.B. Ballard
Chairman, Aeronautical Engr. Dept.
307 Guggenheim Hall
University of Washington
Seattle, Washington 98195

Prof. G.P. Neller
Division of Engineering
Brown University
Providence, Rhode Island 02912

Prof. Werner Goldsmith
Dept. of Mechanical Engineering
Div. of Applied Mechanics
University of California
Berkeley, California 94720

Prof. J.R. Rice
Division of Engineering
Brown University
Providence, Rhode Island 02912

Prof. R.S. Rivlin
Center for the Application of Mathematics
Lehigh University
Bethlehem, Pennsylvania 18015

Library (Code 0384)
U.S. Naval Postgraduate School
Monterey, California 93940

Dr. Francis Cozzarelli
Div. of Interdisciplinary Studies & Resea
School of Engineering
State University of New York
Buffalo, N.Y. 14214

Industry and Research Institutes

Library Services Department
Report Section Bldg. 1203
Argonne National Laboratory
9700 S. Cass Avenue
Argonne, Illinois 60440

Dr. M.C. Junger
Cambridge Acoustical Associates
129 Mount Auburn St.
Cambrige, Massachusetts 02138

Dr. L.H. Chen
General Dynamics Corporation
Electric Boat Division
Groton, Connecticut 06340

Dr. J.E. Greenspon
J.G. Engineering Research Associates
3831 Menlo Drive
Baltimore, Maryland 21215

Dr. S. Batdorf
The Aerospace Corp.
P.O. Box 92957
Los Angeles, California 90009

Dr. E.C. Park
Lockheed Palo Alto Research Laboratory
Dept. 5233, Bldg. 205
3251 Hanover Street
Palo Alto, California 94304

Library
Newport News Shipbuilding and Dry Dock Co.
Newport New, Virginia 23607

Dr. W.F. Borsch
McDonnell Douglas Corporation
5301 Bolsa Ave.
Huntington Beach, California 92647

Dr. H.N. Abramson
Southwest Research Institute
Technical Vice President
Mechanical Sciences
P.O. Drawer 28510
San Antonio, Texas 78284

Dr. R.C. DeMart
Southwest Research Institute
Dept. of Structural Research
PO Drawer 28510
San Antonio, Texas 78284

Dr. M.L. Baron
Weidlinger Associates,
Consulting Engineers
110 East 59th Street
New York, N.Y. 10022

Dr. W.A. von Riesemann
Sandia Laboratories
Sandia Base
Albuquerque, New Mexico 87115

Dr. T.L. Geers
Lockheed Missiles & Space Co.
Palo Alto Research Laboratory
3251 Hanover Street
Palo Alto, California 94304

Dr. J.E. Tucker
Boeing Computer Services, Inc.
P.O. Box 24346
Seattle, Washington 98124

Mr. William Caywood
Code 8B5, Applied Physics Laboratory
8621 Georgia Avenue
Silver Spring, Maryland 20934

Mr. P.C. Durup
Lockheed-California Company
Aeromechanics Dept., 74-43
Burbank, California 91503